A NEW METHOD FOR NONRIGID REGISTRATION OF 3D IMAGES

by

MEHMET ALI AKINLAR

Presented to the Faculty of the Graduate School of

The University of Texas at Arlington in Partial Fulfillment

of the Requirements

for the Degree of

DOCTOR OF PHILOSOPHY

THE UNIVERSITY OF TEXAS AT ARLINGTON

August 2009

To my parents and siblings

Fadime, Namık and Oya, Cüneyt, Hümeyra

ACKNOWLEDGEMENTS

First I would like to thank my supervisor Prof. Guojun Liao for introducing me to the subject of the image registration concept with many interesting application areas. Working with Prof. Liao was not only very informative but also fun. Secondly I would like to thank each member in my thesis committee for their time, and useful advises.

This research was supported by the STEM and graduate dean doctoral fellowships by the graduate school and teaching assistantship by the department of mathematics at UTA. I am happy to take this opportunity to express my thanks to all of my instructors, colleagues, and friends at UTA. It is difficult to list all of their names in here, so I just want to express my deepest gratitude to all of them; thank you and God bless you all.

Finally, my special thanks go to my siblings for their continuous support, and to my parents for their endless patience with me.

June 19, 2009

ABSTRACT

A NEW METHOD FOR NONRIGID REGISTRATION OF 3D IMAGES

MEHMET ALI AKINLAR, Ph.D.

The University of Texas at Arlington, 2009

Supervising Professor: Guojun Liao

In this dissertation we present a novel method for the nonrigid registration of 3D images using a well-established mathematical framework mostly known as the deformation based grid generation method. The deformation based grid generation method is able to generate a grid with desired grid density distribution that is free from grid folding. This method gives direct control over the cell size of the adaptive grid and determines the node velocities directly. The adaptive grid system naturally distributes more grids to deprived areas. The positive monitor function disallows grid folding and provides a mean to control the ratio of the areas between the original and transformed domain. Based on these, we have successfully developed a new non-rigid registration method that has many advantages: Firstly, it is based on a solid mathematical foundation. In particular, it accounts for local volume changes through the divergence of the transformation; and it accounts for local rotation through the curl vector of the transformation. Secondly, the method is based on a linear differential system; its numerical implementation is fast, stable, simple and robust. Thirdly, it does not require to use of any regularization term. Finally, the method is general in the sense that it may be used in any optimization problem that involves motion

estimation. Thus, it has the potential to be the numerical kernel for a wide range of applications.

TABLE OF CONTENTS

LIST OF FIGURES

LIST OF TABLES

CHAPTER 1

INTRODUCTION TO IMAGE REGISTRATION

This dissertation provides a systematic method for the nonrigid registration of 3D images using some techniques of the grid deformation and multigrid optimization. **Image registration** can be defined as a process of determining the optimal transform that maps points from one image to the corresponding points in another image. The images could be of the same or different individuals and imaging modalities, and possibly taken at different distances, angles and times. In basic terms, the image registration can be described as finding a special correspondence between pixels (or voxels) of two images, i.e. finding special grids. Figure 1.1 illustrates an example of template and reference images. Image registration has a broad applications areas in medical and nonmedical images, some of which are to detect tumors and locate diseases, monitoring of changes in an individual, drug discovery, combining information from multiple sources and motion tracking. The most well-known medical imaging modalities are magnetic resonance imaging (MRI), ultrasound (US), computed tomography (CT), single emission computed tomography (SPECT), positron emission tomography (PET), functional MRI (fMRI), X-Ray, diffusion tensor imaging (DTI) and to name a few more.

The methodology behind the image registration concept can be described as to determine the optimal transformations that maximize the "similarity" or minimize the "dissimilarity" between images. The subject of medical image registration, as mentioned above, has broad application areas, some of which are cardiac motion [12], neuro-degenerative brain imaging [13], breast imaging [14], liver and prostate imaging

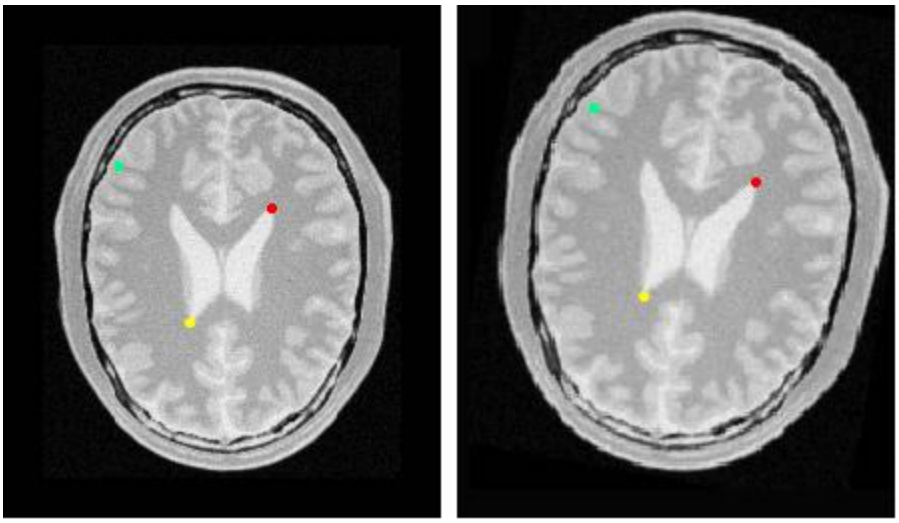

Figure 1.1. An example for template and reference images.

[16], and to name a few more.

Pictures of the brain obtained using some different imaging modalities are illustrated in figure 1.2.

In the literature there are a large amount of work for the problem of nonrigid image registration. For instance, image registration methods based on image correlation have been studied [27]. Medical image registration methods are presented in References ([18], [19], [20], [21]). In Reference [22] the surface based registration methods in medical imaging are reviewed. Some other types of image registration methods are described in ([24], [25], [26]).

In this thesis our aim is to present a systematic method for the nonrigid registration of 3D images using some special techniques of the grid deformation method and multigrid optimization. Our method for nonrigid registration of 3D images is developed by adjusting divergence and curl of an intermediate vector field from which the deformation field is computed using Lagrange multipliers method. Numerical so-

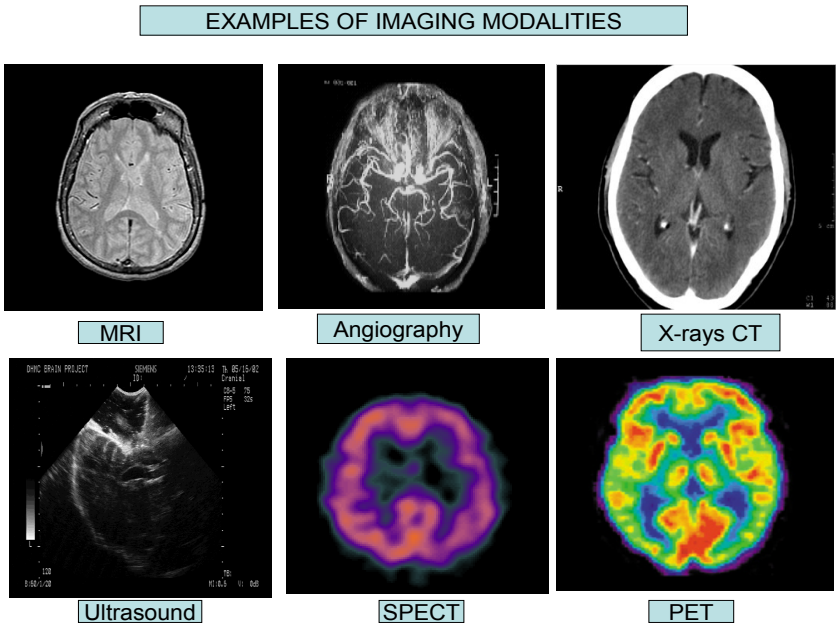

Figure 1.2. Imaging modalities.

lutions of the 3D Poisson equations (decoupling system) is obtained by means of the finite-difference approximations method. The sum of square differences (SSD) is employed as the similarity measure in the cost minimization of the existing registration framework.

In order to better understand the strength of our method, we can list some of the merits of our method as follows:

- It is based on a solid mathematical foundation. In particular, it accounts for local volume changes through the divergence of the transformation; and it accounts for local rotation through the curl vector of the transformation.
- The method is based on a linear differential system; its numerical implementation is fast, stable, simple and robust.

- The method is general in the sense that it may be used in any optimization problem that involves motion estimation. Thus, it has the potential to be the numerical kernel for a wide range of applications.
- It does not require to use of any regularization term.

The main contribution of this thesis to the subject is to present and implement a systematic method for the nonrigid registration of 3D images using some special techniques of the grid deformation and multigrid optimization methods. Although we emphasize the work in 3D case in this thesis, our method works quite well in the registration of 2D images.

This dissertation is organized as follows: In the first chapter we give an introduction to the concept of the image registration. The second chapter considers the image registration problem as a computer programming algorithm and overview the concepts of transformation models, similarity measures, and optimization methods. In the chapter three we describe the grid deformation method and then set up the unconstrained optimization problems using Lagrange multipliers method. In the same chapter we give our method for the nonrigid registration of 3D images. We obtain numerical solution of the optimization problems using finite-difference approximations method. Finally we apply our method to a 3D and a 2D example in our order to illustrate our method.

CHAPTER 2

IMAGE REGISTRATION ALGORITHM

The purpose of this chapter is to describe the image registration as an optimization problem and then overview the components of the image registration algorithm. The registration problem may be phrased as

$$J[R, T; u] := \min \{C_{sim} + \beta C_{reg}\},$$

where C_{sim} is the similarity metric between template and reference images and C_{reg} is the regularization term due to cracks, folding, or other unwanted deformations, and β is the regularization constant. Typical regularizer are the fluid, elastic, diffusive, and curvature smoother.

We can consider the image registration problem as a computer programming algorithm that consists of three major components:

- **Transformation models:** Rigid, Nonrigid.
- **Similarity measures:** Intensity-based, Geometry-based.
- **Optimization methods:** Lagrange multipliers method, Gradient Descent method, Levenberg-Marquardt method, Deterministic Anealing optimization method, Downhill Simplex method, Quasi-Newton, Newton-Raphson method, etc.

2.1 Transformation Models

The goal of transformation models is twofold: Firstly, controlling movement of image features relative to one another to improve the image similarity. Secondly, interpolation between those features. Our method to register 3D images is based on

the deformation based grid generation method which will be described in the next chapter. We divide the transformation models into two main groups: Rigid and nonrigid.

An image transformation is called **rigid**, only if rotations, translations, projections, scaling are used. In particular, if the transformation maps parallel lines onto parallel lines it is called **affine**. Finally, if it maps lines onto curves, it is called **nonrigid**. Next we briefly study each of these transformations.

Rigid Transformations: A rigid image registration mainly consists of rotations, translations, projections, scaling. A rigid transformation maps a line onto a line. Rigid transformations are global and linear, hence they can be represented by matrices. Because affine and projective transformations can be represented by means of matrices, we consider them as a part of rigid transformations. In the literature rigid transformations have found application areas in orthopedic imaging because of the rigid-transformations do not consider soft tissue deformations. Bone growth can be given as a specific example for rigid image registration.

Nonrigid image registration: Nonrigid image registration is an essential tool required for overcoming, for example, soft tissue deformations in medical images. Unlike rigid transformations, nonrigid transformations do not map a line onto a line and, in general, maps a line onto a curve. Nonrigid registrations are mostly local and are not linear, so they can not be represented by means of matrices. The most well-known nonrigid image registrations types are the viscous fluid algorithm ([3], [29], [30], [31], [32]), elastic methods [33], Optical flow methods [34], [35], Thin-Plate Spline and cubic B-spline [37], [12], and the references therein.

2.2 Similarity Metrics

Similarity metric is the most important component in the registration process. Corresponding features in two images may be different from one to another due to the different imaging modalities and imaging conditions. A good similarity measure has to take into account these factors and it should be efficient and stable. We can separate similarity metrics into two major components as intensity-based and geometry based. Next we briefly overview both of these components.

Intensity-based methods: Intensity-based image registration methods match intensity patterns in each image using mathematical or statistical criteria such as entrophy. Although intensity-based image registration methods are more difficult image registration method than geometry based image registration methods, the main advantage of the intensity-based methods is all (or a large portion of) data is used in reference and template images. The most well-known intensity-based method is the mutual information method [38] proposed by Shannon in his theory of information as a measure of entropy of the information shared between two signals.

Geometry-based methods: Geometry-based methods uses some feature values such as local curvature, local maximum/minimum, corner, cusp points etc. in the reference and template images. The most popular geometry-based methods are sum of square differences and cross-correlation.

Sum of Square Differences (SSD): SSD is one of the simplest and most popular similarity measures. In this thesis we use the sum of square difference method in the L^2 norm sense as

$$SSD = \frac{1}{2}\int_{\Omega} \left(To\phi(\mathbf{x}) - R(\mathbf{x})\right)^2 d\mathbf{x},$$

where $\phi(\mathbf{x}) = \mathbf{x}+u(\mathbf{x})$, and $u(\mathbf{x})$ is the displacement. The SSD has several advantages as a similarity metric such as it is fast, robust and simple. SSD provides an indirect

measure of the registration quality: The smaller value of SSD is, the better the images are matched.

2.3 Optimization methods

Optimization methods play significantly important role in computer vision and image analysis. Image registration problem can be formulated as an optimization problem whose goal is to minimize a cost function that consists of a first term that characterizes the similarity between the reference and template images and a regularization term.

The optimization problem for nonlinear registration is ill posed, hence a regularization term C_{reg} is often added to C_{sim}. The optimization problem can be stated as: optimize the cost function $C = C_{sim} + kC_{reg}$, where k is a parameter that represents the tradeoff between the similarity and regularity. In our method we do not need to use any regularization term, which is one of the powers of method. We can list the shortcomings with the regularization term as follows: By adding a regularization term, the resulting transformations do not optimize the similarity measure alone; in fact, if the weighting parameter k is too small, the algorithm will be unstable. If k is too large, the regularity will be too strong and the resulting transformations will not accurately optimize the similarity measure.

Some of the most popular optimization techniques are Lagrange multipliers method, Gradient Descent method, Levenberg-Marquardt method, Deterministic Aneal-ing optimization method, Downhill Simplex method, Quasi-Newton, Newton-Raphson method, etc.

CHAPTER 3

SOME OTHER RELATED METHODS

In this chapter we first overview some other image registration method which uses the grid deformation method and secondly we mention some other important nonrigid image registration methods.

M. Gunzburger and E. Lee proposed [50] a method to solve 2D image registration method using the grid deformation method. Perhaps this is the closest work with our method. Both method uses the GDM. The major differences between our method and [50] are: our method works for 3D case and it does not contain some ordinary differential equations (ODEs) as constraints, but the problem in [50] has been studied for the 2D case and includes some ODEs appearing in the GDM. Optimality systems in each work are different not only in the number of Poisson equations appearing in the optimality system but also in the way of obtaining them. Numerical methods and computational examples are also quite different in these two work.

Another approach for nonrigid image registration using mutual information was introduced in [14]. This is a fast parametric method for nonrigid registration which was developed by adjusting divergence and curl of the intermediate vector field in the grid deformation method from which the deformation field is computed using finite-cental difference method. This method incorporates mutual information with gradient descent optimization into the nonrigid image registration for dynamic contrast-enhanced breast MRI. The authors point out that the multi resolution strategy cuts down the registration time which makes the method feasible for clinical practice. This algorithm is scalable to handle 3D real image data and capable to

register between different image modalities. Mei Yi Chu presented a similar work in her Ph.D thesis [60].

Using deformation based grid generation C.-Y. Hsieh, et al. gave another method [54], namely, "NiRuDeGG" which stands for "Nonrigid Image registration Using Deformation based Grid Generation" which involves no regularization term. The divergence-curl system in the grid deformation method is solved by LSFEM method. C.-Y. Hsieh uses the same ideas in his Ph.D thesis [61]. Another nonrigid image registration method based on Helmholt's theorem was given [55] by the same set of the authors. Helmholtz's theorem states that, with suitable boundary condition, a vector field is completely determined if both of its divergence and curl are specified everywhere. Based on this, the method in [55] was developed. Instead of the displacements of regular control grid points, the curl and divergence at each grid point are employed as the parameters. the authors point out that this method allows for a more efficient optimization scheme over the NiRuDeGG method.

B. B. Avants, et al., presented [56] a Lagrangian reference frame diffeomorphic image and landmark registration method. The algorithm uses the fixed Lagrangian reference frame to define the map between coordinate systems, but also generates and stores the inverse map from the Eulerian to the Lagrangian frame. Computing both maps allows facile computation of both Eulerian and Lagrangian quantities. The authors apply this algorithm to estimating a putative evolutionary change of coordinates between a population of chimpanzee and human cortices. Instead of basing the inter-species study on a single species atlas, the authors diffeomorphically connect the mean shape and intensity templates for each group. The human statistics then map diffeomorphically into the space of the chimpanzee cortex providing a comparison between species. The population statistics show a significant doubling of the relative prefrontal lobe size in humans, as compared to to chimpanzees.

A. Leow et al. point out [57] that maps of local tissue compression or expansion are often computed by comparing magnetic resonance imaging (MRI) scans using nonlinear image registration. The resulting changes are commonly analyzed using tensor-based morphometry to make inferences about anatomical differences, often based on the Jacobian map, which estimates local tissue gain or loss. In [57], A. Leow et al., provide rigorous mathematical analysis of the Jacobian maps, and use them to motivate a new numerical method to construct unbiased nonlinear image registration. First, they argue that log-arithmic transformation is crucial for analyzing Jacobian values representing morphometric differences. They then examine the statistical distributions of log-Jacobian maps by defining the Kullback-Leibler (KL) distance on material density functions arising in continuum-mechanical models. With this framework, unbiased image registration can be constructed by qualifying the symmetric KL-distance between the identity map and the resulting deformation.

M. Miller et al. examines [39] the Euler-Lagrange equations for the solution of the large deformation diffeomorphic metric mapping problem. They compute metric mappings via geodesic flows of diffeomorphisms. Using Lie group ideas A. Trouve construct [40] a distance between deformations defined through a metric given the cost of infinitesimal deformations. Then he proposes a numerical scheme to solve a variational problem involving this distance and leading to a sub-optimal gradient pattern matching. He established its links with fluid models. In another article [41] by A. Trouve and L. Younes analyze a computational problem using the techniques of Lie group actions which has important applications in image understanding and shape analysis.

J. Modersitzki et al. give [51] an image registration method using curvature. They show that their curvature based registration not only produces accurate and smooth solutions but also allows for an automatic rigid alignment.

CHAPTER 4

OPTIMAL CONTROL OF IMAGE REGISTRATION

In this chapter we first describe the grid deformation method and then give the optimal control formulation of image registration using this method. Grid generation plays an essential role in all numerical methods that employ finite differences, finite volume and finite elements. It is the process of discretizing the solution domain into small cells and solutions are obtained at each nodal point. The Grid deformation method (or deformation based grid generation method) that we use in this thesis was outlined by Liao *et al.* [42]. It uses some ideas in Moser's deformation method in differential geometry which constructs a differentiable and invertible transformation between two domains equipped with Riemannian metrics, which deforms the volume element from one to the other. In order to show the strength of this method, we can list the advantages of our method as follows: Instead of adding new nodes to the regions where the need arises and removing the nodes where they are not needed, the adaptive grid generation method moves grid points such that dense grids are resulting in the regions with large variation in solution and coarse grids where the solution variation is small without causing any mesh tangling. The theoretically guaranteed no mesh tangling property of this adaptive grid generation method is achieved by enforcing the Jacobian determinant of the final transformation is equal to a prescribed positive monitor function.

In this thesis we use the adaptive grid generation to register 3D images. By adjusting the divergence and curl parameters, the grid move in a desired way. The positive monitor function $f(x)$ disallows grid folding and provides a mean to control

the ratio of the areas between the original and transformed domain. The flexibility of the adaptive grid allocation could dramatically reduce processing time with quality preserved. The SSD facilitates robust registration between different image modalities. Next we describe the grid deformation method and then set-up the optimization problem using the grid deformation method.

4.1 The Grid Deformation Method

In this section we overview the grid generation method (GDM) that is used for construction of differentiable and invertible transformations to solve mesh adaption problems. A moving-grid algorithm is formulated using the deformation method. The idea of this method is to move the nodes with correct velocities so that the nodal mapping has a desirable Jacobian determinant. This method was developed in ([43], [44]), it was improved in [45] and used with a finite-volume solver in flow calculations in [46]. A 2D dimension version of the method was proposed in [47] and used with a discontinuous Galerkin finite-element method in solving a convection-diffusion problem in [48].

Three versions of the grid deformation method are available in the literature and can be seen in [49].

First version of the grid deformation method: This is one of the steady versions of deformation method where the transformation Jacobian determinant is specified on the old grid $\mathbf{x}$ before adaption.

Description of the problem: Let $\Omega \subset \mathbf{R}^n$ be a bounded convex set with Lipschitz continuous boundary $\partial\Omega$, and a differentiable function $f : \Omega \to \mathbf{R}_+$, namely, monitor (or weight) function, is given such that

$$\int_\Omega (f-1) = 0, \quad \text{or equivalently} \quad \int_\Omega f = |\Omega|,$$

where $|\Omega|$ is the volume of the domain Ω. Find a mapping function

$$\phi_1 : \Omega \to \Omega, \quad \partial\Omega \to \partial\Omega, \tag{4.1.1}$$

such that

$$J(\phi_1) := \det \nabla\phi_1(\mathbf{x}) = f(\mathbf{x}). \tag{4.1.2}$$

Construction of such a map: Using the following steps, we construct ϕ_1.

(1) Find a vector field $u(\mathbf{x})$ which satisfies

$$\begin{aligned} div\, u(\mathbf{x}) &= f(\mathbf{x}) - 1 \quad \text{in} \quad \Omega \\ n \cdot u(\mathbf{x}) &= 0 \quad \text{on} \quad \partial\Omega. \end{aligned}$$

(2) Form a velocity vector field,

$$h(t, \mathbf{x}) = \frac{u(\mathbf{x})}{t + (1-t)f(\mathbf{x})}, \quad 0 < t \leq 1$$

and then, find $\phi_t(\mathbf{x}) = \phi(t, \mathbf{x}), \quad \phi_1(\mathbf{x}) = \phi(1, \mathbf{x})$ by solving the ordinary differential equation

$$\frac{d\phi(t, \mathbf{x})}{dt} = h(t, \phi(t, \mathbf{x})), \quad 0 < t \leq 1 \tag{4.1.3}$$

$$\phi(0, \mathbf{x}) = \mathbf{x}, \tag{4.1.4}$$

In [49], J. Liu proved that the map ϕ_1 constructed in this way satisfies the equality (4.1.2) by showing that the equality given as

$$\frac{\partial H(t, \mathbf{x})}{\partial t} = 0, \quad \text{where} \quad H(t, \mathbf{x}) = J(\phi_t(\mathbf{x}))[t + (1 - tf(\phi_t(\mathbf{x}))]$$

holds for each $t \in [0, 1]$. Notice that f can be chosen any function with the properties described above. In realistic situations, however, f is subject to some additional constraints. Bochev, *et al.* inform us that for example, f should reflect the need for grid refinement of the underlying problem, i.e., one has to choose the mechanism

under which the changes in the exact or approximate solution will be accounted for by the monitor function. Here we give some examples for possible relations between solutions u and the monitor function f:

$$f(t,\mathbf{x}) = \frac{C}{1+\alpha_1|\nabla u(t,\mathbf{x})|^2+\alpha_2|u(t,\mathbf{x})|^2},$$

where C is a normalizing factor that may depend on t. Another possibility is to consider relations of the form

$$f(t,\mathbf{x}) = \frac{C}{\sqrt{1+\alpha|\nabla u(t,\mathbf{x})|^2}},$$

or even simpler monitor function

$$f(t,\mathbf{x}) = \frac{C}{1+|u(t,\mathbf{x})|}.$$

Interested reader can read [49] in conjunction with this thesis to have more information about this version of the grid adaption method and further properties of it.

Second version of the grid deformation method:

This is another static version of deformation method where the transformation Jacobian determinant is specified on the new grid $\phi(\mathbf{x})$ after adaption.

Problem: Given f normalized by $\int_\Omega \frac{1}{f} = |\Omega|$, find a mapping

$$\phi_1 : \Omega \to \Omega, \quad \partial\Omega \to \partial\Omega, \tag{4.1.5}$$

such that

$$J(\phi_1) := \det \nabla\phi_1(\mathbf{x}) = f(\phi_1(\mathbf{x})) \quad \mathbf{x} \in \Omega. \tag{4.1.6}$$

To find such a transformation, we can use the following two steps:

(1) Compute $u(\mathbf{x})$ such that

$$\nabla \cdot u(\mathbf{x}) = 1 - \frac{1}{f(\mathbf{x})}, \quad \mathbf{x} \in \Omega, \tag{4.1.7}$$

and

$$u(\mathbf{x}) \cdot n = 0, \quad \mathbf{x} \in \partial\Omega. \tag{4.1.8}$$

(2) For each fixed node $\mathbf{x}$, solve the ordinary differential equation

$$\frac{d\phi(t,\mathbf{x})}{dt} = h(t,\phi(t,\mathbf{x})), \quad 0 \le t \le 1 \tag{4.1.9}$$

with $\phi(0,\mathbf{x}) = \mathbf{x}$, where

$$h(t,\phi(t,\mathbf{x})) = \frac{u(\phi(t,\mathbf{x}))}{t\frac{1}{f(\phi(t,\mathbf{x}))} + (1-t)}. \tag{4.1.10}$$

Define $\phi_1(\mathbf{x}) = \phi(1,\mathbf{x})$, then $\phi_1(\mathbf{x})$ is the solution. The proof of above approach can be found in [49].

Third version of the grid deformation method: This is the version of deformation method with real time adaption.

Problem: Given a monitor function $f(t,\mathbf{x}) > 0$, normalized with

$$\int_\Omega \frac{1}{f(t,w)} dw = |\Omega(t=0)|,$$

find a mapping $\phi(t,\cdot) : \Omega(t=0) \to \Omega(t)$ such that

$$J(\phi(t,\mathbf{x})) = f(t,\phi(t,\mathbf{x})), \;\; t > 0. \tag{4.1.11}$$

The transformation ϕ can be found by the following two steps:

(1) Find a vector field $u(t,\mathbf{x})$ such that

$$\nabla \cdot u(t,\mathbf{x}) = -\frac{\partial}{\partial t}\frac{1}{f(t,\mathbf{x})} \tag{4.1.12}$$

and $u(t,\mathbf{x}) \cdot n = 0 \quad$ on $\partial\Omega$.

(2) Solve the ordinary differential equation for $\phi(t,\mathbf{x})$

$$\frac{d\phi(t,\mathbf{x})}{dt} = h(t,\phi(t,\mathbf{x})) = f(t,\phi(t,\mathbf{x}))u(t,\phi(t,\mathbf{x})) \tag{4.1.13}$$

In [49] it is shown that the $\phi(t,\mathbf{x})$ found in this way satisfies the equation (4.1.11).

4.2 Nonrigid Registration of 3D Images Using GDM

In this section we study the image registration method using the first version of the grid deformation method. The deformation based grid generation method is able to generate a grid with desired grid density distribution which is free from grid folding. This is achieved by devising a positive monitor function describing the anticipated grid density in the computational domain. Based on it, we have successfully developed a new nonrigid image registration method, which has many advantages. Firstly, the functional to be optimized consists of only one term, a similarity measure, namely, sum of square differences (SSD). Thus, no regularization functional is required in this method. In particular, there is no weight to balance the regularization functional and the similarity functional as commonly required in many nonrigid image registration methods. Nevertheless, the regularity (no mesh folding) of the resulting deformation is theoretically guaranteed by controlling the Jacobian determinant of the transformation. Secondly, because no regularization term is introduced in the functional to be optimized, the resulting deformation field is highly flexible that large deformation frequently experienced in inter-patient or image-atlas registration tasks can be accurately estimated. Detailed description of the nonrigid image registration method based on adaptive grid generation method is presented. Firstly we remark basic notations and definitions.

Notations and definitions:

$$
\begin{aligned}
\mathbf{x} &= (x_1, x_2, x_3),\ u(\mathbf{x}) = (u_1(\mathbf{x}), u_2(\mathbf{x}), u_3(\mathbf{x})),\ v(\mathbf{x}) = (v_1(\mathbf{x}), v_2(\mathbf{x}), v_3(\mathbf{x}), v_4(\mathbf{x})) \\
\phi(\mathbf{x}) &= (\phi_1(\mathbf{x}), \phi_2(\mathbf{x}), \phi_3(\mathbf{x})) \\
&= \mathbf{x} + u(\mathbf{x}) = (x_1 + u_1(\mathbf{x}), x_2 + u_2(\mathbf{x}), x_3 + u_3(\mathbf{x})) : \Omega \subset \mathbf{R}^3 \to \mathbf{R}_+ \\
\nabla &= (\partial_{x_1}, \partial_{x_2}, \partial_{x_3})
\end{aligned}
$$

Theorem 4.2.1 *Let $\Omega \subset \mathbf{R}^3$ be a domain. For ϕ defined above, the equality $J(\phi) \cong 1 + div\,(\varepsilon u) + O(\varepsilon^2)$ holds for every $\varepsilon > 0$ in Ω.*

Proof:

$$
\begin{aligned}
J(\phi) &= \begin{vmatrix} 1+\varepsilon u_{1_{x_1}} & \varepsilon u_{1_{x_2}} & \varepsilon u_{1_{x_3}} \\ \varepsilon u_{2_{x_1}} & 1+\varepsilon u_{2_{x_2}} & \varepsilon u_{2_{x_3}} \\ \varepsilon u_{3_{x_1}} & \varepsilon u_{3_{x_2}} & 1+\varepsilon u_{3_{x_3}} \end{vmatrix}, \\
&= 1 + \varepsilon u_{1_{x_1}} + \varepsilon u_{2_{x_2}} + \varepsilon u_{3_{x_3}} \\
&+ \varepsilon^2 (u_{2_{x_2}} u_{3_{x_3}} - u_{2_{x_3}} u_{3_{x_2}} + u_{1_{x_1}} u_{3_{x_3}} + u_{1_{x_1}} u_{2_{x_2}} - u_{1_{x_2}} u_{2_{x_1}} - u_{1_{x_3}} u_{3_{x_1}}) + \varepsilon^3 J(u), \\
&\cong 1 + \varepsilon u_{1_{x_1}} + \varepsilon u_{2_{x_2}} + \varepsilon u_{3_{x_3}} + O(\varepsilon^2), \\
&= 1 + div\,(\varepsilon u) + O(\varepsilon^2).
\end{aligned}
$$

Lemma 1: The following equalities hold for any scalar function h defined on Ω and a vector $\overrightarrow{v}$.

$$
\begin{aligned}
\int_\Omega \nabla \cdot (h\overrightarrow{v}) &= \int_\Omega \nabla h \cdot \overrightarrow{v} + \int_\Omega h \nabla \cdot \overrightarrow{v} \\
\int_\Omega \nabla \cdot (h\overrightarrow{v}) &= \int_{\partial\Omega} (h\overrightarrow{v}) \cdot \overrightarrow{n} = 0, \text{ if } h = 0 \text{ on } \partial\Omega,
\end{aligned}
$$

where $\overrightarrow{n}$ is the outward and unit normal vector to $\partial\Omega$.

We simplify the first version of the grid deformation method by letting $h(t,x) = h(1,x) = u(x)$. In order to make the transformed template image "similar" to the reference image, we look for a mapping $\phi(t,x)$ which minimizes the L^2-norm of the

difference between $T(\phi(1,x))$ and $R(x)$ over Ω. First we define the functional $J(\phi, f, g)$ as follows:

$$\begin{aligned}
J(\phi, f^1, f^2, f^3, f^4) &= \min \frac{1}{2} \int_\Omega \left[To\phi(\mathbf{x}) - R(\mathbf{x})\right]^2 d\mathbf{x}, \\
\text{subject to} & \\
div\, u &= \nabla \cdot u = u_{1_{x_1}} + u_{2_{x_2}} + u_{3_{x_3}} := f^1, \quad f^1 = f - 1 \\
curl\, u &= (curl_{x_1} u,\, curl_{x_2} u,\, curl_{x_3} u) \\
&= (u_{3_{x_2}} - u_{2_{x_3}}, u_{1_{x_3}} - u_{3_{x_1}}, u_{2_{x_1}} - u_{1_{x_2}}) \\
curl\, u &:= (f^2, f^3, f^4) \\
u &= 0 \quad \text{on} \quad \partial\Omega \\
\partial u &= 0 \quad \text{on} \quad \partial\Omega
\end{aligned}$$

We now look for the controls f^1, f^2, f^3, f^4 and states $\phi(t,x)$ and $u(x)$ such that $J(\cdot,\cdot,\cdot,\cdot,\cdot)$ is minimized subject to the constraints defined above. Our goal here is to minimize $\int_\Omega \left[To\phi(\mathbf{x}) - R(\mathbf{x})\right]^2 d\mathbf{x}$, therefore, we penalize the objective functional with H^1-norms of $f^1 - f^4$. With such a penalization, we are able to show the existence of optimal solutions.

In order to solve this constraint optimization problem, we express it as an unconstraint optimization problem using Lagrange multipliers method where $v = (v_1, v_2, v_3, v_4)$ are Lagrange multipliers. Specializing an abstract theorem concerning the existence of Lagrange multipliers for minimizations on Banach space [51], we obtain the following theorem:

Theorem 4.2.2 *Let V_1 and V_2 be two Hilbert spaces, $\mathcal{F}$ a functional on V_1, and $\mathcal{G}$ a mapping from V_1 to V_2. Assume $\hat{u}$ is a solution of the following constrained minimization problem:*

Find $u \in V_1$ that minimizes $\mathcal{F}(u)$ subject to $\mathcal{G}(u) = 0$. Assume further that the following conditions are satisfied:

(i) $\mathcal{F} : Nbhd(\widehat{u}) \subset V_1 \to \mathbf{R}$ *is Frechet-differentiable at* $\widehat{u}$;

(ii) $\mathcal{G}$ *is continuously Frechet-differentiable at* $\widehat{u}$;

(iii) $\mathcal{G}'(\widehat{u}) : V_1 \to V_2$ *is onto.*

Then, there exists a $\mu \in (V_2)^*$ *such that*

$$\mathcal{F}'(\widehat{u})v - \langle \mu, \mathcal{G}'(\widehat{u})v \rangle = 0, \qquad \forall v \in V_1.$$

PROOF: See [51], Theorem 43.19.

Here, $\langle \cdot, \cdot \rangle$ denotes the duality pairing between V_2 and $(V_2)^*$ and $\mathcal{F}'(\widehat{u})v$ and $\mathcal{G}'(\widehat{u})v$ denote the actions of $\mathcal{F}'(\widehat{u})$ as an operator mapping $v \in V_1$ into $\mathbf{R}$ and $\mathcal{G}'(\widehat{u})$ as an operator mapping $v \in V_1$ into V_2, respectively. We will fit our optimization problem into the above abstract framework.

We penalize $f = (f^1, f^2, f^3, f^4)$. With such a penalization, we, in fact, penalize $v = (v_1, v_2, v_3, v_4)$ and we are able to show the existence of optimal solutions. We apply the Lagrange multiplier method to get the optimality system, the state and adjoint systems and optimality conditions. M. Gunzburger and E. Lee proves [50] the existence of optimal solution and proper Lagrange multipliers using some special techniques of the functional analysis and interested reader can read [50] in conjunction with present work. Let $f := (f^1, f^2, f^3, f^4)$.

$$\begin{aligned} L[u; v; f] = \frac{1}{2}\int_\Omega \left[To\phi(\mathbf{x}) - R(\mathbf{x})\right]^2 d\mathbf{x} + \frac{w_1}{2}\int_\Omega (f^1)^2(\mathbf{x})d\mathbf{x} + \frac{w_2}{2}\int_\Omega (f^2)^2(\mathbf{x})d\mathbf{x} \\ + \frac{w_3}{2}\int_\Omega (f^3)^2(\mathbf{x})d\mathbf{x} + \frac{w_4}{2}\int_\Omega (f^4)^2(\mathbf{x})d\mathbf{x} + \int_\Omega v_1(\mathbf{x})(div\, u(\mathbf{x}) - f^1(\mathbf{x}))d\mathbf{x} \\ + \int_\Omega v_2(\mathbf{x})(curl_{x_1}\, u(\mathbf{x}) - f^2(\mathbf{x}))d\mathbf{x} + \int_\Omega v_3(\mathbf{x})(curl_{x_2}\, u(\mathbf{x}) - f^3(\mathbf{x}))d\mathbf{x} \\ + \int_\Omega v_4(\mathbf{x})(curl_{x_3}\, u(\mathbf{x}) - f^4(\mathbf{x}))d\mathbf{x}. \end{aligned}$$

Solution of the Lagrange functional satisfies the optimality system which consists of state equations, costate equations, and the optimality conditions.

State Equations: The state equations are obtained from $L_{v_1} = 0, \quad L_{v_2} = 0, \quad L_{v_3} = 0$ and $L_{v_4} = 0$.

$$\begin{aligned} L_{v_1} &= \frac{d}{d\varepsilon}\Big|_{\varepsilon=0} L[v_1 + \varepsilon\delta v_1] = \frac{d}{d\varepsilon}\Big|_{\varepsilon=0} \int_\Omega (v_1 + \varepsilon\delta v_1)(div\, u - f^1) \\ &= \int_\Omega \delta v_1 (div\, u - f^1) = 0 \quad \text{for every} \quad \delta v_1. \end{aligned}$$

Then,

$$div\, u(\mathbf{x}) = f^1(\mathbf{x}). \tag{4.2.14}$$

$$\begin{aligned} L_{v_2} &= \frac{d}{d\varepsilon}\Big|_{\varepsilon=0} L[v_2 + \varepsilon\delta v_2] = \frac{d}{d\varepsilon}\Big|_{\varepsilon=0} \int_\Omega (v_2 + \varepsilon\delta v_2)(curl_{x_1}\, u - f^2) \\ &= \int_\Omega \delta v_2 (curl_{x_1}\, u - f^2) = 0 \quad \text{for every} \quad \delta v_2. \end{aligned}$$

Then,

$$curl_{x_1}\, u(\mathbf{x}) = f^2(\mathbf{x}). \tag{4.2.15}$$

$$\begin{aligned} L_{v_3} &= \frac{d}{d\varepsilon}\Big|_{\varepsilon=0} L[v_3 + \varepsilon\delta v_3] = \frac{d}{d\varepsilon}\Big|_{\varepsilon=0} \int_\Omega (v_3 + \varepsilon\delta v_3)(curl_{x_2}\, u - f^3) \\ &= \int_\Omega \delta v_3 (curl_{x_2}\, u - f^3) = 0 \quad \text{for every} \quad \delta v_3. \end{aligned}$$

Then,

$$curl_{x_2}\, u(\mathbf{x}) = f^3(\mathbf{x}). \tag{4.2.16}$$

$$\begin{aligned} L_{v_4} &= \frac{d}{d\varepsilon}\Big|_{\varepsilon=0} L[v_4 + \varepsilon\delta v_4] = \frac{d}{d\varepsilon}\Big|_{\varepsilon=0} \int_\Omega (v_4 + \varepsilon\delta v_4)(curl_{x_3}\, u - f^4) \\ &= \int_\Omega \delta v_4 (curl_{x_3}\, u - f^4) = 0 \quad \text{for every} \quad \delta v_4. \end{aligned}$$

Then,

$$curl_{x_3}\, u(\mathbf{x}) = f^4(\mathbf{x}). \tag{4.2.17}$$

In summary, the state equations are given by

$$\begin{aligned} L_{v_1} = 0 &\Rightarrow div\, u = f^1, \\ L_{v_2} = 0 &\Rightarrow curl_{x_1}\, u = f^2, \\ L_{v_3} = 0 &\Rightarrow curl_{x_2}\, u = f^3, \\ L_{v_4} = 0 &\Rightarrow curl_{x_3}\, u = f^4. \end{aligned}$$

Costate equations: The costate equations are obtained by solving the equations $L_{u_1} = 0,\ L_{u_2} = 0$ and $L_{u_3} = 0$.

$$\begin{aligned} L_{u_1} &= \frac{d}{d\varepsilon}\Big|_{\varepsilon=0}\Big[\frac{1}{2}\int_\Omega [T(\mathbf{x} + (u_1(\mathbf{x}) + \varepsilon\delta u_1(\mathbf{x}), u_2(\mathbf{x}), u_3(\mathbf{x}))) - R(\mathbf{x})]^2 \\ &+ \int_\Omega v_1(div\,(u_1 + \varepsilon\delta u_1, u_2, u_3) - f^1) + \int_\Omega v_3(curl_{x_2}\,(u_1 + \varepsilon\delta u_1, u_2, u_3) - f^3) \\ &+ \int_\Omega v_4(curl_{x_3}\,(u_1 + \varepsilon\delta u_1, u_2, u_3) - f^4)\Big] \\ &= \int_\Omega (T(\mathbf{x} + u(\mathbf{x})) - R(\mathbf{x}))\, T_{\phi_1}\, \delta u_1 + \int_\Omega v_1(\delta u_1)_{x_1} + \int_\Omega v_3(\delta u_1)_{x_3} + \int_\Omega v_4(-\delta u_1)_{x_2} \\ &= \int_\Omega (T(\mathbf{x} + u(\mathbf{x})) - R(\mathbf{x}))\, T_{\phi_1}\, \delta u_1 + \int_\Omega (v_1, -v_4, v_3)\cdot\nabla\delta u_1 \\ &= \int_\Omega [(T - R)\, T_{\phi_1}\, \delta u_1 - \nabla\cdot(v_1, -v_4, v_3)\delta u_1] \ \text{(by lemma 1 and } h = \delta u_1 = 0 \,\text{on}\, \partial\Omega) \\ &= \int_\Omega [(T - R)\, T_{\phi_1} - \nabla\cdot(v_1, -v_4, v_3)]\, \delta u_1 = 0 \text{ for every } \delta u_1, \end{aligned}$$

which gives us the first costate equation

$$\nabla\cdot(v_1, -v_4, v_3) = (T - R)T_{\phi_1}. \tag{4.2.18}$$

$$
\begin{aligned}
L_{u_2} &= \frac{d}{d\varepsilon}\Big|_{\varepsilon=0}[\frac{1}{2}\int_\Omega [T(\mathbf{x}+(u_1,u_2(\mathbf{x})+\varepsilon\delta u_2(\mathbf{x}),u_3(\mathbf{x})))-R(\mathbf{x})]^2 \\
&+ \int_\Omega v_1(div\,(u_1,u_2+\varepsilon\delta u_2,u_3)-f^1) \\
&+ \int_\Omega v_2(curl_{x_1}\,(u_1,u_2+\varepsilon\delta u_2,u_3)-f^3) \\
&+ \int_\Omega v_4(curl_{x_3}\,(u_1,u_2+\varepsilon\delta u_2,u_3)-f^4)] \\
&= \int_\Omega (T(\mathbf{x}+u(\mathbf{x}))-R(\mathbf{x}))\,T_{\phi_2}\,\delta u_2+\int_\Omega v_1(\delta u_2)_{x_2}+\int_\Omega v_2(-\delta u_2)_{x_3}+\int_\Omega v_4(\delta u_2)_{x_1} \\
&= \int_\Omega (T(\mathbf{x}+u(\mathbf{x}))-R(\mathbf{x}))\,T_{\phi_2}\,\delta u_2+\int_\Omega (v_4,v_1,-v_2)\cdot\nabla\delta u_2 \\
&= \int_\Omega [(T-R)\,T_{\phi_2}\,\delta u_2-\nabla\cdot(v_4,v_1,-v_2)\delta u_2]\ \text{(by lemma 1 and}\quad h=\delta u_2=0\,\text{on}\,\partial\Omega) \\
&= \int_\Omega [(T-R)\,T_{\phi_2}-\nabla\cdot(v_4,v_1,-v_2)]\,\delta u_2=0\ \text{for every}\ \delta u_2,
\end{aligned}
$$

which gives us the second costate equation

$$\nabla\cdot(v_4,v_1,-v_2)=(T-R)T_{\phi_2}. \tag{4.2.19}$$

$$
\begin{aligned}
L_{u_3} &= \frac{d}{d\varepsilon}\Big|_{\varepsilon=0}[\frac{1}{2}\int_\Omega [T(\mathbf{x}+(u_1,u_2,u_3(\mathbf{x})+\varepsilon\delta u_3(\mathbf{x})))-R(\mathbf{x})]^2 \\
&+ \int_\Omega v_1(div\,(u_1,u_2,u_3+\varepsilon\delta u_3)-f^1) \\
&+ \int_\Omega v_2(curl_{x_1}\,(u_1,u_2,u_3+\varepsilon\delta u_3)-f^2)] \\
&+ \int_\Omega v_3(curl_{x_2}\,(u_1,u_2,u_3+\varepsilon\delta u_3)-f^3) \\
&= \int_\Omega T(\mathbf{x}+u(\mathbf{x})-R(\mathbf{x}))\,T_{\phi_3}\,\delta u_3+\int_\Omega v_1(\delta u_3)_{x_3}+\int_\Omega v_2(\delta u_3)_{x_2}+\int_\Omega v_3(-\delta u_3)_{x_1} \\
&= \int_\Omega T(\mathbf{x}+u(\mathbf{x})-R(\mathbf{x}))\,T_{\phi_3}\,\delta u_3+\int_\Omega (-v_3,v_2,v_1)\cdot\nabla\delta u_3 \\
&= \int_\Omega [(T-R)\,T_{\phi_3}\,\delta u_3-\nabla\cdot(-v_3,v_2,v_1)\delta u_3]\ \text{(by lemma 1 and}\quad h=\delta u_3=0\,\text{on}\,\partial\Omega) \\
&= \int_\Omega [(T-R)\,T_{\phi_3}-\nabla\cdot(-v_3,v_2,v_1)]\,\delta u_3=0\ \text{for every}\ \delta u_3,
\end{aligned}
$$

which gives us the third costate equation

$$\nabla\cdot(-v_3,v_2,v_1)=(T-R)T_{\phi_3}. \tag{4.2.20}$$

Hence, the costate equations are given by

$$\begin{aligned}(T-R)\,T_{\phi_1} &= \nabla\cdot(v_1,-v_4,v_3),\\ (T-R)\,T_{\phi_2} &= \nabla\cdot(v_4,v_1,-v_2),\\ (T-R)\,T_{\phi_3} &= \nabla\cdot(-v_3,v_2,v_1).\end{aligned}$$

Optimality conditions: The optimality conditions are obtained by solving the equations $L_{f^1}=0,\ L_{f^2}=0,\ L_{f^3}=0$ and $L_{f^4}=0$.

$$\begin{aligned}L_{f^1} &= \frac{d}{d\varepsilon}\Big|_{\varepsilon=0}\left[\frac{w_1}{2}\int_\Omega (f^1+\varepsilon\delta f^1)^2+\int_\Omega v_1(div\,u-(f^1+\varepsilon\delta f^1))\right]\\ &= \int_\Omega w_1 f^1\delta f^1 - v_1\delta f^1\\ &= \int_\Omega (w_1f^1-v_1)\delta f^1 = 0 \text{ for every } \delta f^1,\end{aligned}$$

which gives us the first optimality condition

$$w_1 f^1 = v_1. \tag{4.2.21}$$

$$\begin{aligned}L_{f^2} &= \frac{d}{d\varepsilon}\Big|_{\varepsilon=0}\left[\frac{w_2}{2}\int_\Omega (f^2+\varepsilon\delta f^2)^2+\int_\Omega v_2(curl_{x_1}\,u-(f^2+\varepsilon\delta f^2))\right]\\ &= \int_\Omega (w_2f^2-v_2)\delta f^2 = 0 \text{ for every } \delta f^2,\end{aligned}$$

which gives us the second optimality condition

$$w_2 f^2 = v_2. \tag{4.2.22}$$

$$\begin{aligned}L_{f^3} &= \frac{d}{d\varepsilon}\Big|_{\varepsilon=0}\left[\frac{w_3}{2}\int_\Omega (f^3+\varepsilon\delta f^3)^2+\int_\Omega v_3(curl_{x_2}\,u-(f^3+\varepsilon\delta f^3))\right]\\ &= \int_\Omega (w_3f^3-v_3)\delta f^3 = 0 \text{ for every } \delta f^3,\end{aligned}$$

which gives us the third optimality condition

$$w_3 f^3 = v_3. \tag{4.2.23}$$

$$\begin{aligned} L_{f^4} &= \frac{d}{d\varepsilon}\Big|_{\varepsilon=0}\left[\frac{w_4}{2}\int_\Omega (f^4+\varepsilon\delta f^4)^2 + \int_\Omega v_4(curl_{x_3}\, u - (f^4+\varepsilon\delta f^4))\right] \\ &= \int_\Omega (w_4 f^4 - v_4)\delta f^4 = 0 \text{ for every } \delta f^4, \end{aligned}$$

which gives us the fourth optimality condition

$$w_4 f^4 = v_4. \tag{4.2.24}$$

Hence, the optimality conditions are given by

$$\begin{aligned} L_{f^1} = 0 &\Rightarrow w_1 f^1 = v_1, \\ L_{f^2} = 0 &\Rightarrow w_2 f^2 = v_2, \\ L_{f^3} = 0 &\Rightarrow w_3 f^3 = v_3, \\ L_{f^4} = 0 &\Rightarrow w_4 f^4 = v_4. \end{aligned}$$

Now we write the optimality system as follows:

State equations:

$$\begin{aligned} div\, u &= f^1, \\ curl_{x_1}\, u &= f^2, \\ curl_{x_2}\, u &= f^3, \\ curl_{x_3}\, u &= f^4. \end{aligned}$$

Costate equations:

$$\begin{aligned} (T-R)\, T_{\phi_1} &= \nabla\cdot(v_1, -v_4, v_3), \\ (T-R)\, T_{\phi_2} &= \nabla\cdot(v_4, v_1, -v_2), \\ (T-R)\, T_{\phi_3} &= \nabla\cdot(-v_3, v_2, v_1). \end{aligned}$$

Optimality conditions:

$$\begin{aligned} w_1 f^1 &= v_1, \\ w_2 f^2 &= v_2, \\ w_3 f^3 &= v_3, \\ w_4 f^4 &= v_4. \end{aligned}$$

Decoupling:

We will solve this system of equations by multi-grid optimization method using the Poisson equations defined in the following way:

Define

$$F_1 := f^1, \quad F_2 := f^2, \quad F_3 := f^3, \quad F_4 := f^4.$$

Then, the state equations give us

$$\begin{aligned} \Delta u_1 &= F_{1_{x_1}} + F_{3_{x_3}} - F_{4_{x_2}}, \\ \Delta u_2 &= F_{1_{x_2}} - F_{2_{x_3}} + F_{4_{x_1}}, \\ \Delta u_3 &= F_{1_{x_3}} + F_{2_{x_3}} - F_{3_{x_1}}. \end{aligned}$$

Define $G := (G_1, G_2, G_3)$ as

$$\begin{aligned} G_1 &:= (T - R)\, T_{\phi_1}, \\ G_2 &:= (T - R)\, T_{\phi_2}, \\ G_3 &:= (T - R)\, T_{\phi_3}. \end{aligned}$$

Then, we write the costate equations as

$$\begin{aligned} \nabla \cdot (v_1, -v_4, v_3) &= G_1, \\ \nabla \cdot (v_4, v_1, -v_2) &= G_2, \\ \nabla \cdot (-v_3, v_2, v_1) &= G_3. \end{aligned}$$

Further, using the optimality conditions and the the fact that $div\, curl\, u = 0$, where $curl\, u = (f^2, f^3, f^4)$, we have

$$\frac{1}{w_2}\, v_{2_{x_1}} + \frac{1}{w_3}\, v_{3_{x_2}} + \frac{1}{w_4}\, v_{4_{x_3}} = 0$$

Hence, we write the costate equations as

$$\begin{aligned}
G_1 &= v_{1_{x_1}} - v_{4_{x_2}} + v_{3_{x_3}}, \\
G_2 &= v_{4_{x_1}} + v_{1_{x_2}} - v_{2_{x_3}}, \\
G_3 &= -v_{3_{x_1}} + v_{2_{x_2}} + v_{1_{x_3}}, \\
0 &= \frac{1}{w_2}\, v_{2_{x_1}} + \frac{1}{w_3}\, v_{3_{x_2}} + \frac{1}{w_4}\, v_{4_{x_3}},
\end{aligned}$$

from which we write the Poisson equations as

$$\begin{aligned}
\Delta v_1 &= G_{1_{x_1}} + G_{2_{x_2}} + G_{3_{x_3}}, \\
\Delta v_2 &= -G_{2_{x_3}} + G_{3_{x_2}} + \left(1 - \frac{w_2}{w_4}\right) v_{4_{x_1\, x_3}} + \left(1 - \frac{w_2}{w_3}\right) v_{3_{x_1\, x_2}}, \\
\Delta v_3 &= G_{1_{x_3}} - G_{3_{x_1}} + \left(1 - \frac{w_3}{w_4}\right) v_{4_{x_2\, x_3}} + \left(1 - \frac{w_3}{w_2}\right) v_{2_{x_1\, x_2}}, \\
\Delta v_4 &= -G_{1_{x_2}} + G_{2_{x_1}} + \left(1 - \frac{w_4}{w_3}\right) v_{3_{x_2\, x_3}} + \left(1 - \frac{w_4}{w_2}\right) v_{2_{x_1\, x_3}}.
\end{aligned}$$

For simplicity, letting $w_2 = w_3 = w_4$, we get

$$\begin{aligned}
\Delta v_1 &= G_{1_{x_1}} + G_{2_{x_2}} + G_{3_{x_3}}, \\
\Delta v_2 &= -G_{2_{x_3}} + G_{3_{x_2}}, \\
\Delta v_3 &= G_{1_{x_3}} - G_{3_{x_1}}, \\
\Delta v_4 &= -G_{1_{x_2}} + G_{2_{x_1}}.
\end{aligned}$$

4.3 Numerical Implementation

A simple iterative scheme for solving the state and costate equations and optimality conditions in a decoupled manner is follows:

- Suppose that at the k^{th} step, we have found $(f^1)^k$, (where f^1 =div u) and $((f^2)^k, (f^3)^k, (f^4)^k)$, where (curl u= (f^2, f^3, f^4)).
- Obtain $u^k = (u_1^k, u_2^k, u_3^k)$ from the state equations.
- Obtain $v_1^k, v_2^k, v_3^k, v_4^k$ from the costate equations.
- Next get new controls $((f^1)^{k+1}, (f^2)^{k+1}, (f^3)^{k+1}, (f^4)^{k+1})$ from the optimality conditions.
- Normalize controls and repeat the same process until the error condition is satisfied or as many as iteration you want.

Although there are a few sophisticated methods to solve this type of problems numerically, we use the finite-difference method to solve the Poisson equations appearing in the decoupling system. Let us consider a general Poisson equation given by $\Delta u = rhs$, where rhs stands for a function. Then, in 3D case using finite-differences method we can express this Poisson equation in a discrete form as

$$\frac{u_{i-1,j,k}-2u_{i,j,k}+u_{i+1,j,k}}{\Delta x^2} + \frac{u_{i,j-1,k}-2u_{i,j,k}+u_{i,j+1,k}}{\Delta y^2} + \frac{u_{i,j,k-1}-2u_{i,j,k}+u_{i,j,k+1}}{\Delta z^2} = rhs_{i,j,k}$$

Suppose that $\Delta x = \Delta y = \Delta z = h$, then we can represent any interior point as

$$u_{i,j,k} = \frac{1}{6}\left(u_{i-1,j,k} + u_{i+1,j,k} + u_{i,j-1,k} + u_{i,j+1,k} + u_{i,j,k-1} + u_{i,j,k+1} - h^2 \times rhs_{i,j,k}\right).$$

The resulting system of linear algebraic equations is then solved by using successive overrelaxation method in the following way:

$$\begin{aligned} \widetilde{u}_{i,j,k} &= \frac{1}{6}\left(u_{i-1,j,k}^{new} + u_{i+1,j,k}^{new} + u_{i,j-1,k}^{new} + u_{i,j+1,k}^{new} + u_{i,j,k-1}^{new} + u_{i,j,k+1}^{new} - h^2 \times rhs_{i,j,k}\right) \\ u_{i,j,k}^{new} &= (1-\mu)u_{i,j,k}^{old} + \mu\widetilde{u}_{i,j,k} \end{aligned}$$

The cube has 8 corners, 12 edges and 6 faces on the boundary. On the boundary, the second type boundary condition (Neumann boundary condition) is implemented by $\frac{\partial u}{\partial n} = 0$. For instance, we implement the corner $(0, 0, 0)$ as

$$\begin{aligned} u_{0,0,0} &= \frac{1}{6}\left(u_{-1,0,0} + u_{1,0,0} + u_{0,-1,0} + u_{0,1,0} + u_{0,0,-1} + u_{0,0,-1} + u_{0,0,1} - h^2 \times rhs_{0,0,0}\right) \\ &= \frac{1}{6}\left(2u_{1,0,0} + 2u_{0,1,0} + 2u_{0,0,1} - h^2 \times rhs_{0,0,0}\right) \end{aligned}$$

Here we used the facts that

$$\begin{aligned} \frac{u_{1,0,0} - u_{-1,0,0}}{2\Delta x} = 0 &\Rightarrow u_{1,0,0} = u_{-1,0,0} \\ \frac{u_{0,1,0} - u_{0,-1,0}}{2\Delta y} = 0 &\Rightarrow u_{0,1,0} = u_{0,-1,0} \\ \frac{u_{0,0,1} - u_{0,0,-1}}{2\Delta z} = 0 &\Rightarrow u_{0,0,1} = u_{0,0,-1} \end{aligned}$$

We can implement the other corners in the same way. It is clear that

$$\begin{aligned} \frac{u_{i,1,0} - u_{i,-1,0}}{2\Delta y} = 0 &\Rightarrow u_{i,1,0} = u_{i,-1,0} \\ \frac{u_{i,0,1} - u_{i,0,-1}}{2\Delta z} = 0 &\Rightarrow u_{i,0,1} = u_{i,0,-1} \end{aligned}$$

$$\begin{aligned} u_{i,0,0} &= \frac{1}{6}\left(u_{i-1,0,0} + u_{i+1,0,0} + u_{0,-1,0} + u_{0,1,0} + u_{0,0,-1} + u_{0,0,1} - h^2 \times rhs_{0,0,0}\right) \\ &= \frac{1}{6}\left(u_{i-1,0,0} + u_{i+1,0,0} + u_{0,1,0} + u_{0,1,0} + u_{0,0,1} + u_{0,0,1} - h^2 \times rhs_{0,0,0}\right) \\ &= \frac{1}{6}\left(u_{i-1,0,0} + u_{i+1,0,0} + 2u_{0,1,0} + 2u_{0,0,1} - h^2 \times rhs_{i,0,0}\right) \end{aligned}$$

Implementing the other edges in the similar way, we have the following:

$$\begin{aligned} u_{i,0,j} &= \frac{1}{6}\left(u_{i-1,0,j} + u_{i+1,0,j} + u_{i,-1,j} + u_{i,1,j} + u_{i,0,j-1} + u_{i,0,j+1} - h^2 \times rhs_{i,0,j}\right) \\ &= \frac{1}{6}\left(u_{i-1,0,j} + u_{i+1,0,j} + u_{i,1,j} + u_{i,1,j} + u_{i,0,j-1} + u_{i,0,j+1} - h^2 \times rhs_{i,0,j}\right) \\ &= \frac{1}{6}\left(u_{i-1,0,j} + u_{i+1,0,j} + 2u_{i,1,j} + u_{i,0,j-1} + u_{i,0,j+1} - h^2 \times rhs_{i,0,j}\right) \end{aligned}$$

Because the other boundary faces are implemented in the same way, we skip the details inhere.

CHAPTER 5

COMPUTATIONAL EXAMPLES

Example 1: Our first example is in 3D and we use $16 \times 16 \times 16$ initial uniform grid on reference and template images. We define the reference and template images in 3D as follows:

$$reference = \begin{cases} 10, & \text{d}\leq 0; \\ 9.5 + 5(0.1 + 1.5d), & 0 \leq d \leq 2; \\ 25, & 2 \leq d. \end{cases}$$

where

$$d = \sqrt{(x-8)^2 + (y-8)^2 + (z-9)^2} - 3.$$

$$template = \begin{cases} 10, & \text{d}\leq 0; \\ 9.5 + 5(0.1 + 3d), & 0 \leq d \leq 1; \\ 25, & 1 \leq d. \end{cases}$$

where

$$d = \sqrt{(x-8)^2 + (y-8)^2 + (z-9)^2} - 2.$$

After iterating SSD 230 steps (in less than 2 minutes), SSD is reduced from 140.9 to 3.2 which shows one of the strengths of our method.

Example 2: Our second example is in 2D and we are using 64×64 initial uniform grid on reference and template images. We define the reference and template images in 2D as follows:

Table 5.1. Example in 3D: SSD vs Iterations

Iterations	SSD
1	149.6
10	145.1
30	132.3
50	120.1
70	108.7
90	96.3
110	83.5
130	70.1
150	55.9
170	43.1
190	30.2
210	16.4
230	3.3

$$reference = \begin{cases} 10, & \text{d}\leq 0; \\ 9.5 + 5(0.1 + 1.5d), & 0 \leq d \leq 2; \\ 25, & 2 \leq d. \end{cases}$$

where

$$d = \sqrt{1.6(x-30)^2 + (y-30)^2} - 12$$

$$template = \begin{cases} 10, & \text{d}\leq 0; \\ 9.5 + 5(0.1 + 3d), & 0 \leq d \leq 1; \\ 25, & 1 \leq d. \end{cases}$$

where

$$d = \sqrt{(x-35)^2 + 1.5(y-35)^2} - 7.$$

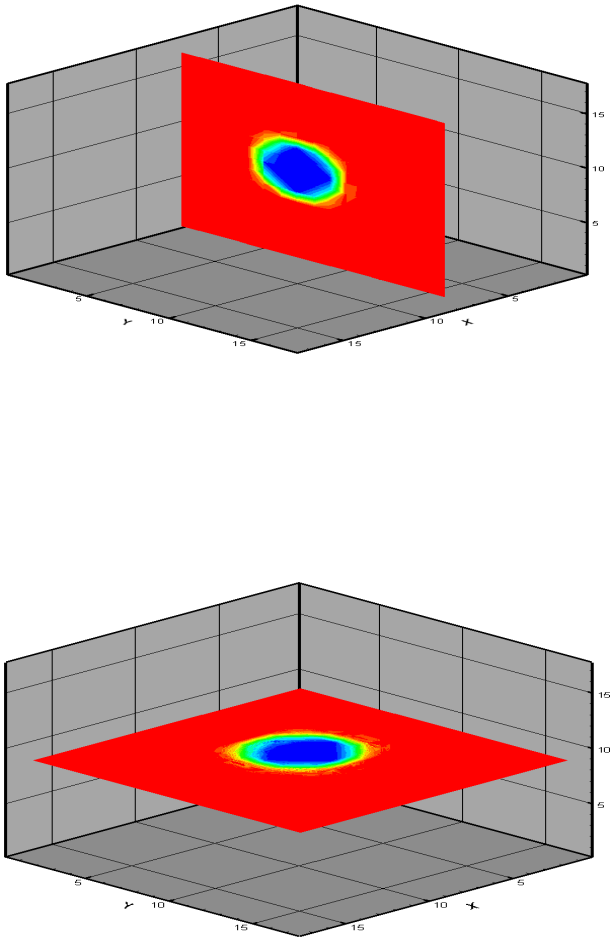

Figure 5.1. Slices through x and z-axes.

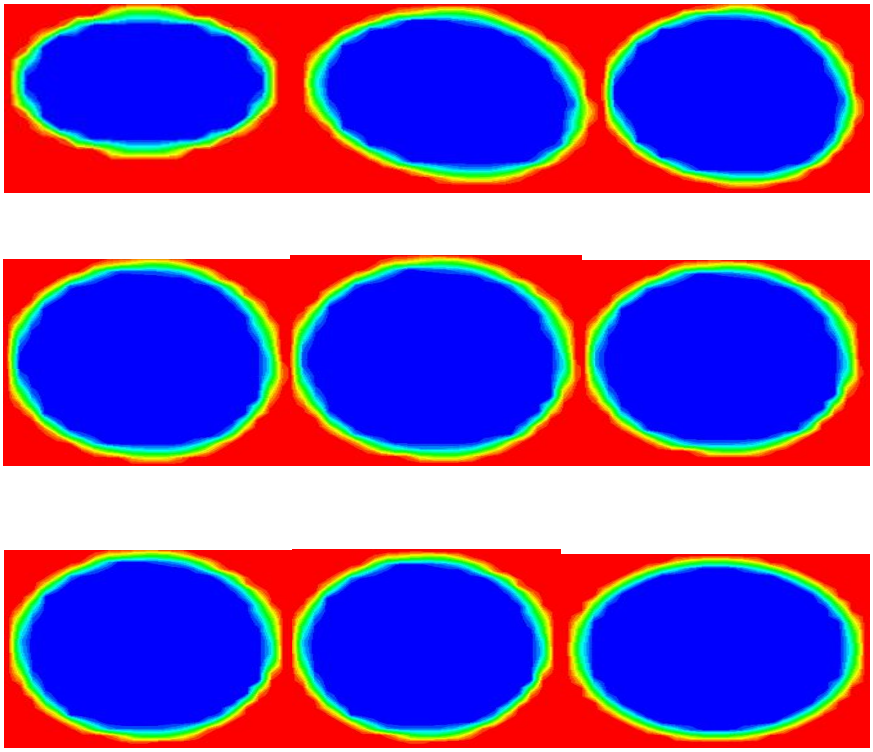

Figure 5.2. Representation of 2d registration.

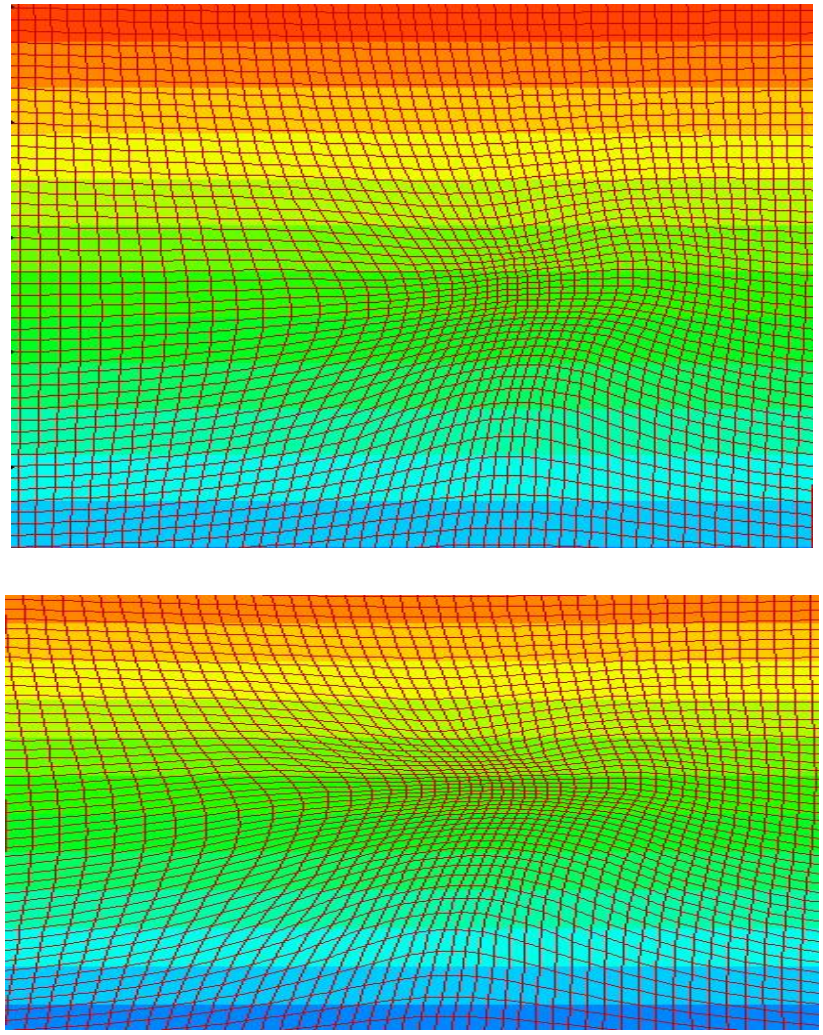

Figure 5.3. Adaptive grids after 1 step.

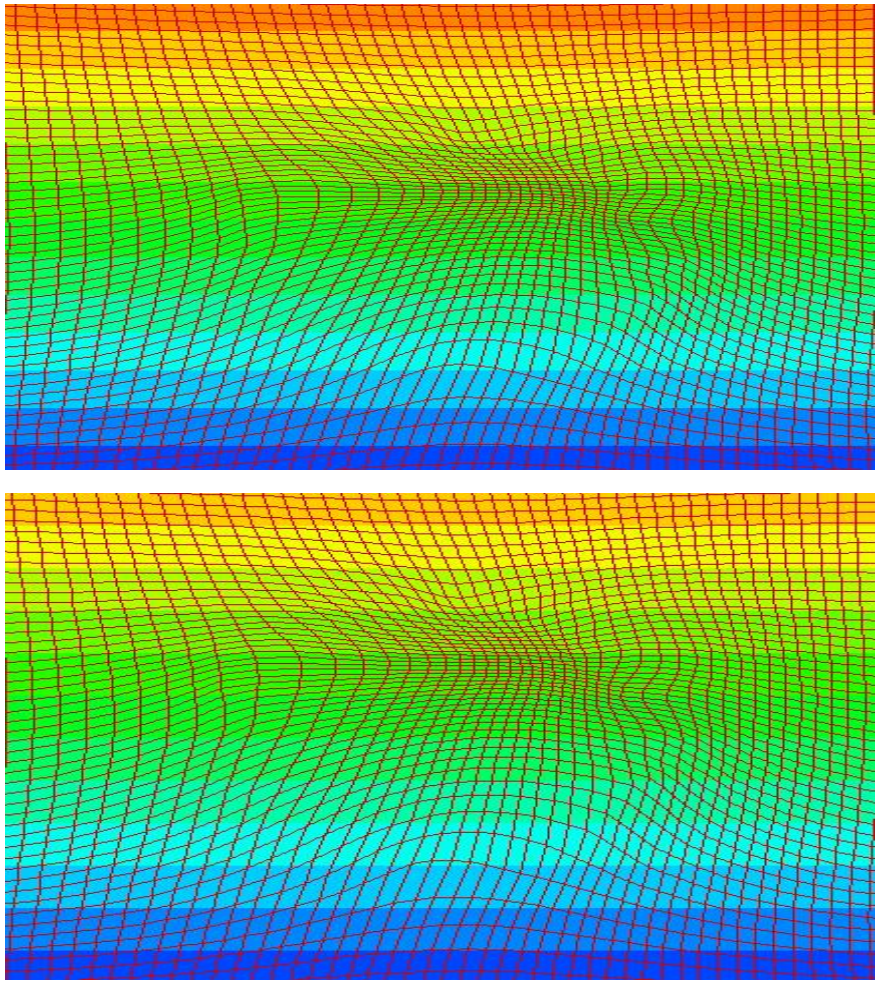

Figure 5.4. Adaptive grids after 10 steps.

CHAPTER 6

SUMMARY

Nonrigid image registration is a very important branch of the image processing concept. It has broad application areas in medical and non-medical imaging. For instance, it can be used in analyzing local anatomical variations that exist between images acquired from different individuals or atlases. It can serve as a powerful tool for combining information from multiple sources, monitoring changes in an individual, detect tumors and locate disease, motion correction and many more. In medical imaging, nonrigid image registrations are mostly used in modeling of soft tissue deformations. Major challenges in the nonrigid image registration are: noisy and distorted data, 3D large nonlinear deformation, occlusion, finding reliable similarity measures for inter-subjects and multi-modalities, high computational costs, etc.

In this thesis we have presented a systematic method for the nonrigid registration of 3D medical images using some special techniques of the grid deformation and multi-grid optimization methods. The Lagrange Multipliers method to write the constrained optimization problem as an unconstrained optimization problem was used. Poisson equations appearing in the optimality system were solved by means of finite-difference approximations method. Preliminary experiments show promising results and great potential for future extension. We can list some of the merits of our method as follows:

- It is based on a solid mathematical foundation. In particular, it accounts for local volume changes through the divergence of the transformation; and it accounts for local rotation through the curl vector of the transformation.

- The method is based on a linear differential system; its numerical implementation is fast, stable, simple and robust.
- The method is general in the sense that it may be used in any optimization problem that involves motion estimation. Thus, it has the potential to be the numerical kernel for a wide range of applications.
- It does not require to use of any regularization term.

In the future, the proposed algorithm is going to be applied to some other possible applications.

REFERENCES

[1] R. Bajcsy and S. Kovacic, *Multiresolution elastic matching,* Computer vision, graphics, and image processing, **46(1),** 1–21, (1989).

[2] P. Thevenaz and M. Under, *Optimization of mutual information for multi-resolution image registration,* IEEE trans. on image processing, **9,** 2083–2099 (2000).

[3] G. E. Christensen, *Deformable shape models for anatomy,* Washington university Ph.D theis, (1994).

[4] C. G. M. Bro-Nielsen, *Fast fluid registration of medical images,* Visualization in Biomedical computing, VBC'96, 267–276, (1996).

[5] A. Collington, F. Maes, D. Delaere, D. Vandermeulen, P. Suetens, and G. Marchal, *Automated multi-modality image registration based on information theory,* Inf. proc. in medical imaging, Kluwer Academic, 263–374, (1995).

[6] C. Meyer, J. Boes, B. Kim, R. Bland, P. Wahl, K. Zasadny, P. Kison, K. Koral, and K. Frey, *Demonstration of accuracy and clinical versatilty of mutual information for automatic multimodality image fusion using affine and thin plate spline warped geometric deformations,* Medical image analysis, **1,** 195–206, (1997).

[7] F. Maes, A. Collington, D. Delaere, D. Vandermeulen, P. Suetens, and G. Marchal, *Multimodality image registration by maximization of mutual information,* IEEE trans. on medical imaging, **16,** 187–198 (1997).

[8] S. Periaswamy and H. Farid, *Elastic registration in the presence of intensity variations,* IEEE transactions on medical imaging, **22(7),** 865–874 (2003).

[9] W. I. Wells, P. Viola, H. Atsumi, S. Nakajima, and R. Kikinis, *Multimodal volume registration by maximization of mutual information,* Medical image analysis, **1,** 35–51 (1996).

[10] C. Studholme, D. Hill, and D. Hawkes, *Automated 3-d registration of mr and ct images of the head,* Medical image analysis, **1,** 163–175 (1996).

[11] M. Jenkinson and S. Smith, *A global optimization method for robust affine registration of brain images,* Medical image analysis, **5,** 143–156 (2001).

[12] N. A. Ablitt, J. Gao, J. Keegan, L. Stegger, D. N. Firmin, and G.-Z. Yang, *Predictive Cardiac Motion Modeling and Correction with Partial Least Squares Regression,* Transactions on Medical Imaging, **23,** No: 10, 1315–1324 (2004).

[13] B. B. Avants, C. L. Epstein, M. Grossman, and J. C. Gee, *Symmetric Diffeomorphic Image Registration with Cross-Corelation: Evaluating Automated Labeling of Elderly and Neurodegenerative Brain,* Medical Image Analysis, **12,** 26–41 (2008).

[14] M. Chu, H. Chen, C. Hsieh, T. Lin, H. Hsiao, G. G. Liao, and Q. Peng, *Adaptive Grid Generation Based Non-rigid Image Registration using Mutual Information for Breast MRI,* Journal of Signal Processing Systems, DOI 10.1007/s11265-008-0193-7, (2008).

[15] G. G. Liao, X. Cai, D. Fleitas, X. Luo, J. Wang, and J. Xue, *Optimal Control Approach to Data Set Alignment,* Applied Mathematics Letters, **21,** 898–905 (2008).

[16] G. Niculescu, D. J. Forand, and J. Nosher, *Non-rigid Registration of the Liver in Consecutive CT Studies for Assessment of Tumor Response to Radiofrequency Ablation,* 29th Annual International Conference of the IEEE Engineering in Medicine and Biology Society, 856–859 (2007).

[17] M. De Craene, et al., *Multimodal nonrigid registration using a stochastic gradient approximation ,* IEEE International Symposium on Biomedical Imaging: Nano to Macro, **2,** 1459 - 1462 (2004).

[18] D.L.G. Hill, P.G. Batchelor, M. Holden, D.J. Hawkes, *Medical image registration,* Physics in Medicine and Biology, **46,** R1R45 (2001).

[19] H. Lester, S.R. Arridge, *A survey of hierarchical non-linear medical image registration,* Pattern Recognition, **32,** 129149 (1999).

[20] J.B.A. Maintz, M.A. Viergever, *A survey of medical image registration,* Medical Image Analysis, **2,** 1-36, (1998).

[21] P.A. van den Elsen, E.-J.D. Pol, M.A. Viergever, *Medical image matching-a review with classification,* IEEE Engineering in Medicine and Biology, **12,** 2639, (1993).

[22] M.A. Audette, F.P. Ferrie, T.M. Peters, *An algorithmic overview of surface registration techniques for medical imaging,* Medical image Analysis, **4,** 201217, (2000).

[23] L. Ding, A. Goshtasby, M. Satter, *Volume image registration by template matching,* Image and Vision Computing, **19,** 821832, (2001).

[24] L.M.G. Fonseca, B.S. Manjunath, *Registration techniques for multisensor remotely sensed imagery,* Photogrammetric Engineering and Remote Sensing, **62,** 10491056, (1996).

[25] E. Gülch, *Results of test on image matching of ISPRS WG,* ISPRS Journal of Photogrammetry and Remote Sensing, **46,** 118, (1991).

[26] J. le Moigne, *First evaluation of automatic image registration methods,* Proceedings of the International Geoscience and Remote Sensing Symposium IGARSS98, Seattle, Washington, 315317, (1998).

[27] B.K. Ghaffary, A.A. Sawchuk, *A survey of new techniques for image registration and mapping,* Proceedings of the SPIE: Applications of Digital Image Processing, **432,** 222239, (1983).

[28] L.G. Brown, *A survey of image registration techniques,* ACM Computing Surveys, **24,** 326376, (1992).

[29] X. Xu and R. D. Dony, *Fast fluid registration using inverse filtering for non-rigid image registration,* Biomedical Imaging: Nano to Macro, 2006. 3rd IEEE International Symposium on Volume , **6-9,** 470-473, (April-2006).

[30] L.G. Brown, *A survey of image registration techniques, ACM Computing Surveys,* **24,** 326376 (1992).

[31] H. Lester and S.R. Arridge, *Summarising fluid registration by thin-plate spline warps with many landmarks,* In Proceedings of Medical Image Understanding and Analysis (MIUA97), Oxford, (1997).

[32] G. Wollny and F. Kruggel, *Computational cost of nonrigid registration algorithms based on fluid dynamics,* IEEE Transactions on Medical Imaging, **21,** 946952, (2002).

[33] C. Davatzikos, *Spatial transformation and registration of brain images using elastically deformable models,* Comput. Vis. Image understand, **66,** 207–222, (1997).

[34] S.S. Beuchemin and J.L. Barron, *The computation of optical flow, ACM Computing Surveys,* **27,** 433467, (1995).

[35] D. J. Fleet and Y. Weiss, *Optical flow estimation,* Mathematical models for Computer Vision: The handbook, **15,** Springer, 239-258, (2005).

[36] J. Ashburner, P. Neelin, D. L. Collins, A.Evans and K. Friston, *Incorporating prior knowledge into image registration,* Neuroimage, **6,** 344-352, (1997).

[37] C. M. Swingen, R. T. Seethamraju, M. J.-Herold, *Feedback-assisted three-dimensional reconstruction of the left ventricle with MRI,* Journal of Magnetic Resonance Imaging, **17(5),** 528 - 537, (2003).

[38] C. E. Shannon, *A Mathematical Theory of Communication,* Bell System Technical Journal, *27,* 379423 and 623656, July and October, (1948).

[39] M. F. Beg, M. I. Miller, A. Trouve and L. Younes, *Computing large deformation metric mappings via geodesic flows of diffeomorphisms,* International journal of computer vision, *61(2),* 139-157, (2005).

[40] A. Trouve, *Diffeomorphisms group and pattern matching in image analysis,* International journal of computer vision, **28(3),** 213-221, (1998).

[41] A. Trouve and L. Younes, *Metamorphoses through Lie group action,* Foundations of computational mathematics, 173-198, (2005).

[42] G. Liao and D. Anderson, *A new approach to grid generation,* Applicable analysis, **44(3),** 285-298, (1992).

[43] G. Liao and J. Su, *A direct method in Dacorogna-Moser's approach of grid generation problems,* Applied Analysis, **45,** (1993).

[44] G. Liao and J. Su, *Grid generation via deformation,* Applied mathematics letters, **5,** (1992).

[45] G. Liao, T. Pan, and J. Su, *A numerical grid generator based on Moser's deformation method,* Num. Met. PDE, **10,** (1994).

[46] F. Liu, S. Ji, and G. Liao, *An adaptive grid method with cell-volume control and its applications to Euler flow calculations,* SIAM J. Sci. comput, **20,** (1998).

[47] G. Liao and J. Su, *A moving grid method for (1+1) dimension,* Applied mathematics letters, **8,** (1995).

[48] C. W. Shu and S. Osher, *Efficient implementation of essentailly non-oscillatory shock capturing scheme,* Journal of mathematical physics, **77,** (1988).

[49] J. Liu, *New development of the deformation method,* Ph.D thesis, The university of Texas at Arlington, (2006).

[50] E. Lee and M. Gunzburger, *An optimal control formulation of an image registration problem,* preprint, (2009).

[51] E. Zeidler, *Nonlinear analysis and its applications,* **III,** Springer, New York, (1988).

[52] J. M. Fitzpatrick, D. L. G. Hill, Y. Shyer, et al., *Visual assessment of the accuracy of retrospective registration of MR and CT images of the brain,* IEEE Transactions medical imaging, **17,** 571-585, (1998).

[53] M. Chu *et al.*, *Adapative Grid Generation Based Nonrigid Image registration using Mutual Information for Breast MRI,* Journal of signal processing systems, **54(1-3),** 45 - 63, (2009).

[54] C. Hsieh *et al.*, *On the development of a new nonrigid image registration using deformation based grid generation,* Medical Imaging 2008: Image processing, Proc. of SPIE, **6914,** 69140W1-69140W12, (2008).

[55] H. Hsiao et al., *A new parametric nonrigid image registration method based on Helmholtz's theorem,* Medical Imaging 2008: Image processing, Proc. of SPIE, **6914,** 69142W1-69140W11, (2008).

[56] B. B. Avants, P. T. Schoenemann and J. C. Gee, *Lagrangian frame diffeomorphic image registration: Morphometric comparision of human and chimpanzee cortex,* Medical Image Analysis, **10,** 397 - 412, (2006).

[57] A. D. Leow *et al.*, *Statistical Properties of Jacobian Maps and the Realization of Unbiased Large-Deformation nonlinear image Registration,* IEEE Transactions on Medical Imaging, **26,** 822 - 832, (2007).

[58] M. I. Miller, *Computational anatomoy: shape, growth, and atrophy comparison via diffeomorphisms,* NeuroImage, **23,** 19 – 33, (2004).

[59] E. Haber and J. Modersitzki, *A Scale Space Method for Volume Preserving Image Registration,* Scale Space and PDE Methods in Computer Vision, **3495,** 1611-3349, (2005).

[60] M. Yi Chu, *Mutual Information Based Nonrigid Image Registration Using Adaptive Grid Generation: GPU Implementation and Application to Breast MRI,* Ph.D thesis, UT, Arlington, (2008).

[61] C.-Y. Hsieh, *Nonrigid Image Registration by the Deformation Based Grid Generation*, Ph.D thesis, UT, Arlington, (2008).

BIOGRAPHICAL STATEMENT

Mehmet Ali Akinlar was born in Eskişehir, Turkey, in 1976. He received his B.Sc. and M.Sc. degrees from Anadolu University, Turkey, in 1999 and 2002, respectively. He completed his second M.Sc. thesis at McMaster University, Canada, in 2005, and his Ph.D at The University of Texas at Arlington (UTA), in 2009. His all degrees are in Mathematics. He has been a teaching and research assistant in several mathematics courses at Anadolu and McMaster Universities for 6 years and worked as a course instructor at UTA from January 2007 to August 2009. His research interest lies in variational methods, optimization, numerical computations and exact and numerical solutions of partial differential equations.